Technical Report 422

Radar Location for Complete Coverage of Representative Threat-Volumes

S. D. Ewing, Jr.
D. Caldwell

15 August 1966

Prepared for the Advanced Research Projects Agency
under Electronic Systems Division Contract AF 19(628)-5167 by

Lincoln Laboratory
MASSACHUSETTS INSTITUTE OF TECHNOLOGY
Lexington, Massachusetts

The work reported in this document was performed at Lincoln Laboratory, a center for research operated by Massachusetts Institute of Technology. This research is a part of Project DEFENDER, which is sponsored by the U.S. Advanced Research Projects Agency of the Department of Defense; it is supported by ARPA under Air Force Contract AF 19(628)-5167 (ARPA Order 498).

MASSACHUSETTS INSTITUTE OF TECHNOLOGY

LINCOLN LABORATORY

RADAR LOCATION FOR COMPLETE COVERAGE OF REPRESENTATIVE THREAT-VOLUMES

S. D. EWING, JR.

Group 44

D. CALDWELL

Group 41

TECHNICAL REPORT 422

15 AUGUST 1966

LEXINGTON MASSACHUSETTS

ABSTRACT

A radar is constrained to scan within a volume of space modeled as a cone with the apex at the radar. The threat-volume is modeled as the frustum of a right-circular cone inverted on a flat earth with a vertical axis and with the height equal to the maximum acquisition altitude. Threatening objects can enter anywhere within this volume above some specified minimum re-entry angle that determines the apex angle of the frustum. The problem solved is that of finding the minimum surface range of the radar that permits the entire frustum volume to be included within the given scanning cone. The important special case of a point impact zone (base radius of frustum $\rightarrow 0$) is also discussed. Results are presented showing how this minimum distance is affected by changing (1) the minimum re-entry angle, (2) the scan angle, (3) the maximum radar acquisition altitude, and (4) the impact-zone radius. Effects of earth curvature are also discussed. These results are useful as one aspect of optimizing radar location in terminal defense studies.

Accepted for the Air Force
Franklin C. Hudson
Chief, Lincoln Laboratory Office

CONTENTS

Abstract	iii
List of Symbols	vi
I. INTRODUCTION	1
II. DISCUSSION OF SOLUTION AND RESULTS	1
A. Flat-Earth Approximation	13
B. Conclusions	15
III. MATHEMATICAL ANALYSIS	15
APPENDIX A – Hyperbolic Boundary Curve	23
APPENDIX B – Critical Re-entry Angle γ^*	25
APPENDIX C – Cosine Product Identity	27
APPENDIX D – "Dip Region" Solution for D_{min} and α_D	28
APPENDIX E – Minimum Coverage Development	29

LIST OF SYMBOLS

h	Maximum radar acquisition altitude, i.e., height of the threat-volume
R_o	Radius of the circular impact zone
γ	Minimum re-entry angle of the RV
β	Arbitrary azimuth approach angle of the RV
φ	Half-angle of the conical radar scan region
α	Radar coverage cone boresight axis elevation angle
r	Normalized impact-zone radius ($r = R_o/h$)
D	Separation distance (surface range) between the radar location and the impact-zone center
D_{min}	Minimum separation distance (surface range) for total threat-volume coverage
α_D	Radar boresight elevation angle when D is a minimum (D_{min})
YH	Minimum altitude above the impact zone for total radar coverage of the threat-volume

RADAR LOCATION FOR COMPLETE COVERAGE OF REPRESENTATIVE THREAT-VOLUMES

I. INTRODUCTION

One of the basic problems in the design of a ballistic missile defense system is radar placement. The radar must be located in a strategic position to acquire the re-entry vehicles (RV's) at a predetermined altitude and track the threatening objects until they are either destroyed or reach their destination in a defended zone (e.g., city, missile base, etc.). The threat-volume is modeled as the frustum of an inverted cone with its axis perpendicular to the earth. Its height h equals the maximum radar acquisition altitude, and its smaller circular base of radius R_o represents the impact zone. Re-entry vehicle trajectories, which will be assumed to be straight lines, may have any re-entry angle larger than a specified minimum. The minimum re-entry angle γ also determines the apex angle $(90 - \gamma)$ of the threat-volume frustum. The RV may enter the modeled threat-volume at any azimuth angle β and any re-entry angle larger than γ. A flat earth is assumed.

A single-faced array radar is constrained to electronically scan a volume of space modeled as a cone of half-angle φ with the apex at the radar. The problem consists of finding the minimum surface range of the radar that permits the entire threat-volume frustum to be included within the given scanning cone (Fig. 1).

The mathematical solution to this complex geometry problem has useful applications to terminal defense systems studies as one aspect of optimizing radar location about the defended zone. In particular, results are presented in Sec. II showing how this minimum distance varies parametrically with (a) re-entry angle, (b) scan angle, (c) impact-zone radius, and (d) maximum radar acquisition altitude. Effects of earth curvature are also discussed.

Sec. III presents a detailed mathematical solution and discussion of various important special cases such as the "point impact zone" wherein $R_o \to 0$ in the general case.

II. DISCUSSION OF SOLUTION AND RESULTS

Figures 2(a) and (b) show that if a plane, A-B-C-D, parallel to the flat earth (x-y plane) is allowed to cut the radar coverage cone at a height z, the boundary of this intersection (Radar Coverage Boundary Curve)† is a major factor in determining threat-volume coverage. In particular, threat-volume coverage‡ merely requires that (a) the larger frustum circular boundary (threat-lid) remain completely internal to the RCBC at the maximum coverage (acquisition)

† Hereafter referred to as RCBC.

‡ See Sec. III.

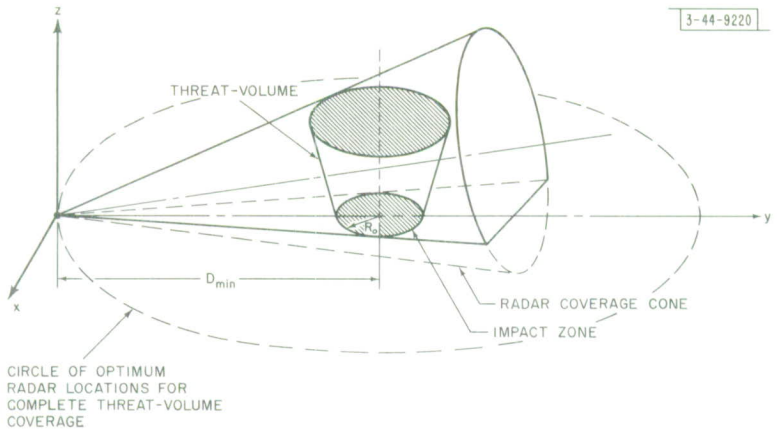

Fig. 1. Radar coverage of threat-volume.

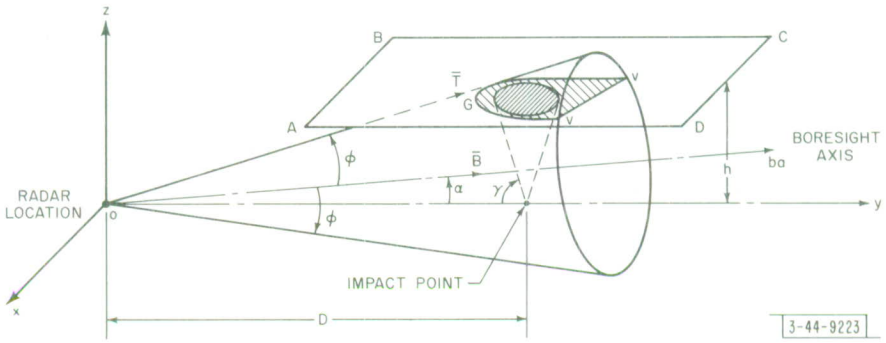

(a)

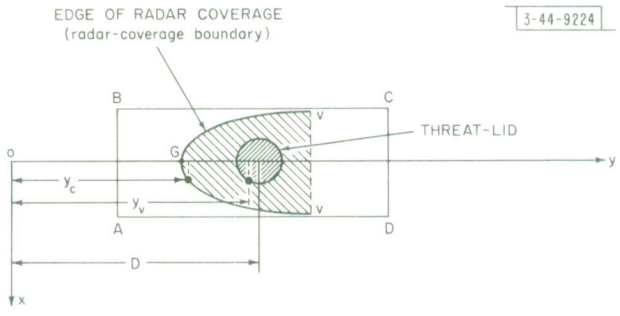

(b)

Fig. 2. Radar coverage boundary curve geometry.

altitude h, and (b) that the circular impact-zone boundary curve remain internal to the RCBC at z = 0 while we minimize the separation distance D between the radar location and the impact-zone center. It can be shown† for particular values of h, φ, and α that two regional solutions result for complete radar coverage of a threat-volume with a finite circular impact area. The point impact-zone solutions ($R \to 0$) are shown to be special cases of these solutions.

Case 1 – Circular Impact Zone ($R_o \neq 0$)

Region 1:– Examination of Fig. 2 reveals that D will be a minimum when α is less than φ and both the threat-lid and the impact zone are tangent to the RCBC at z = h and 0, respectively. The value of D is a minimum in this situation because either tilting the radar coverage cone up or down will result in inadequate coverage of the impact zone or the threat-lid. In this region, the solutions for D_{min} and α_D, the optimum boresight elevation angle, are given by

$$D_{min} = h \csc\varphi \left\{ r^2 + \frac{[(\cot\gamma + r)^2 + 1 - r^2]^2}{(2 \sec\varphi)^2} \right\}^{1/2}$$

$$\alpha_D = \cot^{-1} \left\{ \cot^2\varphi + \left[\frac{2r \csc\varphi}{(\cot\gamma + r)^2 + 1 - r^2} \right]^2 \right\}^{1/2}$$

for

$$\gamma^* < \gamma < 90°$$

where

$$\gamma^* = \cot^{-1}\left(\sqrt{2 \sec^2\varphi + r^2 - 1} - r \right)$$

$$r = R_o/h \quad .$$

Region 1 is designated the "tangent region" because both the threat-lid and the impact-zone boundary curves are tangent to the RCBC at z = h and 0, respectively.

Region 2:– For values of $0 < \gamma \leqslant \gamma^*$, the radar coverage cone can be dipped down and moved closer until the threat-lid is tangent to the RCBC at the widest portion of the radar coverage cone, i.e., across its diameter [see Figs. 3(a) and (b)]. Complete coverage is provided in this configuration because (a) the radar is as close as possible to the impact zone, (b) tilting the radar coverage cone either up or down will cause inadequate coverage of the threat-lid, and (c) the angular range on γ assures impact-zone coverage. D_{min} and α_D are given by

$$D_{min} = h \sqrt{\frac{(\cot\gamma + r)^2 - \tan^2\varphi}{\sin\varphi}} = \frac{h \cot\alpha_D}{\cos^2\varphi}$$

$$\alpha_D = \tan^{-1} \left[\frac{\tan\varphi}{\cos\varphi \sqrt{(\cot\gamma + r)^2 - \tan^2\varphi}} \right]$$

for

$$0 < \gamma \leqslant \gamma^*$$

in region 2, which is referred to as the "dip region."

---

† See Sec. III.

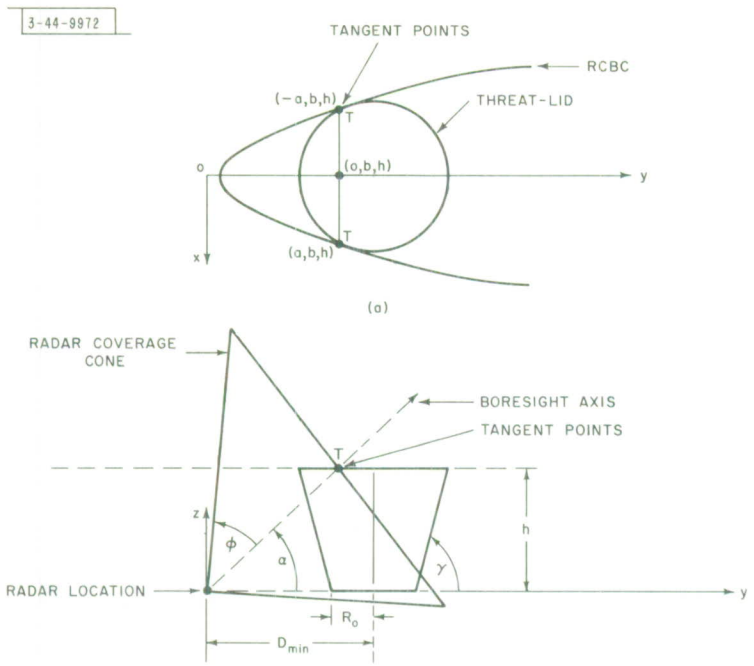

Fig. 3. "Dip region" for circular impact zone. (a) Top view; (b) side view.

Results:– Table I summarizes the expressions for D_{min} and $\alpha_{D'}$ while Figs. 4(a) through (c) present plots of D_{min}/h, the normalized separation distance, for various normalized impact-zone radii ($r = R_o/h$) and radar scan half-angles. Break points between the regional solution of regions 1 and 2 are indicated by circles. The associated radar boresight axis elevation angles are given in Figs. 5(a) through (c). The plots of D_{min}/h illustrate the advantage of using a wide scan radar system to cover a particular impact-zone size. A closer examination of the plots for constant φ (let $\varphi = 60°$) and constant γ (let $\gamma = 20°$) reveals that the increase in D_{min}/h is less than 11 percent for a 100-percent change in R_o/h. This result indicates that, if a wide scan radar system is used, the impact-zone size does not significantly affect the normalized separation distance.

Case 2 – Point Impact Zone ($R_o = 0$)

The point impact-zone coverage results consist of four regional solutions which are obtained from the general solutions of Case 1.

Two of the regional solutions in this case, namely the "tangent region" and the "dip region" (when $R_o = 0$) are straightforward and result from setting $R_o = 0$ in the general solutions of Case 1 for D_{min} and $\alpha_{D'}$. The two remaining solutions are described as follows.

"Trivial Region":– If the minimum re-entry is large enough, the radar can be located at the impact point. This impact-point radar location ($D_{min} = 0$) is possible because the radar coverage cone is large enough to cover completely the threat-volume and, in particular, the threat-lid as shown in Fig. 6(a).

"Lip Region":– The radar coverage cone apex has to be located a distance D from the impact point for complete threat-volume coverage if the radar scan coverage cone is not large

TABLE 1

CASE 1 – FINAL RESULTS FOR THE CIRCULAR IMPACT ZONE ($R_o \neq 0$)

	D_{min}/h	α_D
$\gamma^* \leqslant \gamma < 90°$ "tangent region"	$\csc\phi \left\{ r^2 + \left[\dfrac{(\cot\gamma + r)^2 + 1 - r^2}{2\sec\phi} \right]^2 \right\}^{1/2}$ (19a)	$\cot^{-1} \left\{ \cot^2\phi + \left[\dfrac{2r\csc\phi}{(\cot\gamma + r)^2 + 1 - r^2} \right]^2 \right\}^{1/2}$ (19b)
$0 < \gamma < \gamma^*$ "dip region"	$\dfrac{\sqrt{(\cot\gamma + r)^2 - \tan^2\phi}}{\sin\phi}$ (20a) or $\dfrac{\cot\alpha_D}{\cos^2\phi}$ (20b)	$\tan^{-1}\left[\dfrac{\tan\phi}{\cos\phi\sqrt{(\cot\gamma + r)^2 - \tan^2\phi}} \right]$ (20c)

Note: $\gamma = \cot^{-1}\left[\sqrt{2\sec^2\phi + r^2 - 1} - r\right]$

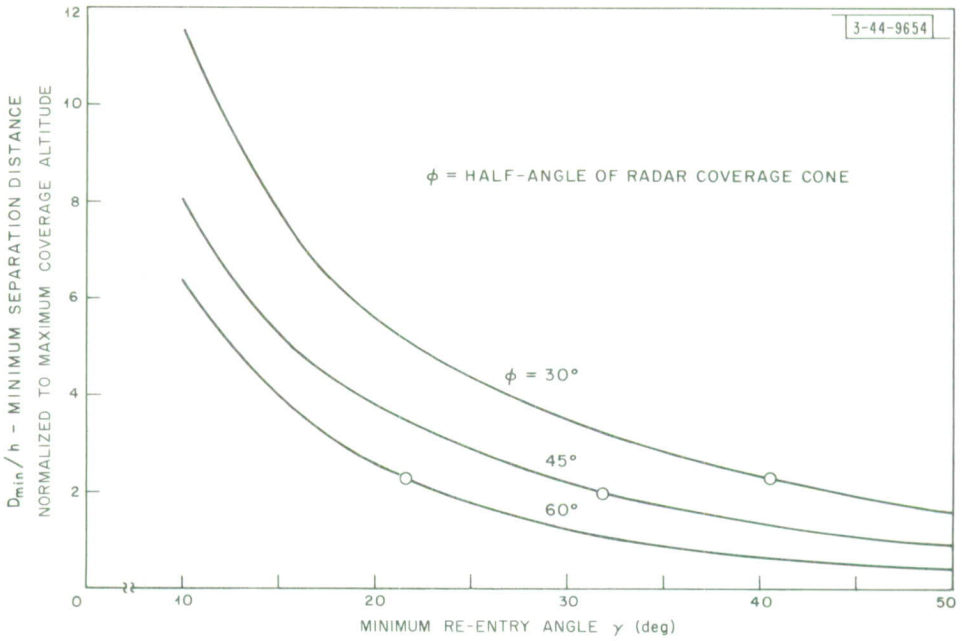

(a) R/h = 0. 125.

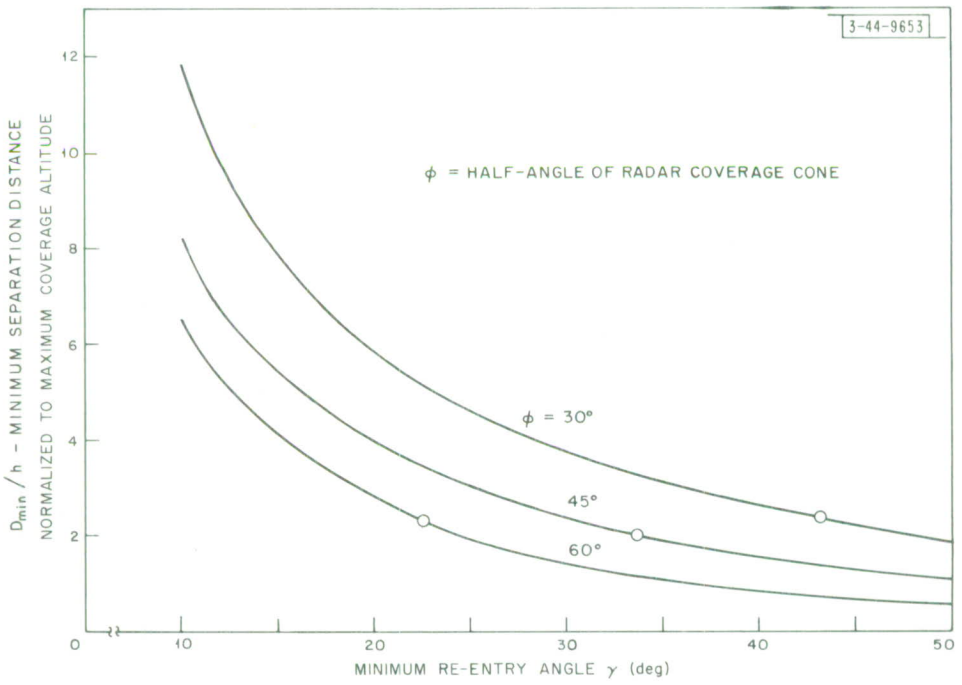

(b) R/h = 0. 250.

Fig. 4(a-c). Circular impact-zone minimum separation distance vs minimum re-entry angle.

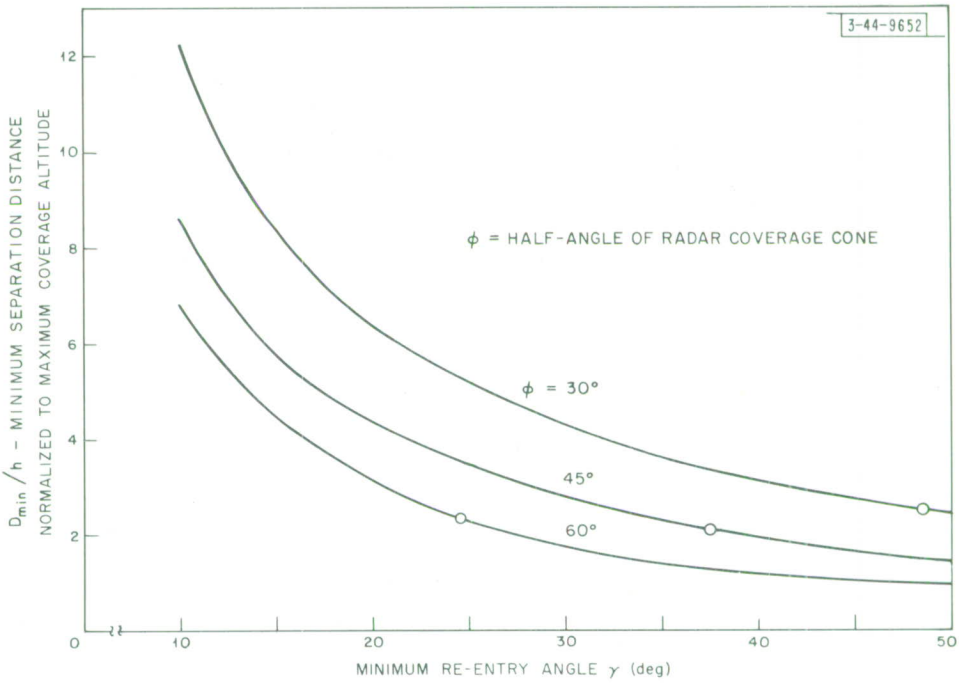

(c) R/h = 0.500.

Fig. 4. Continued.

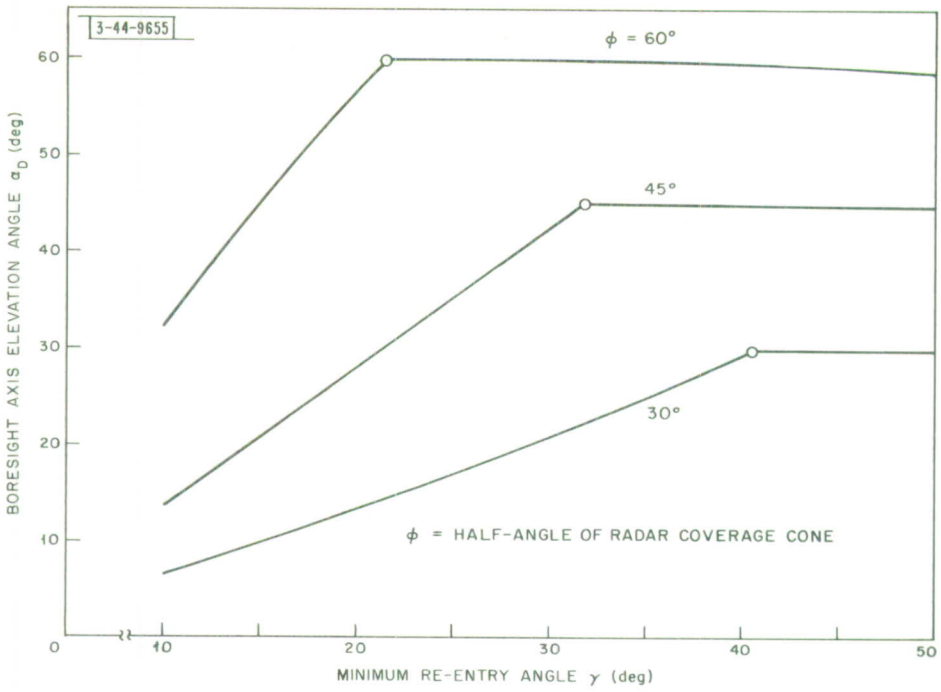

(a) R/h = 0.125.

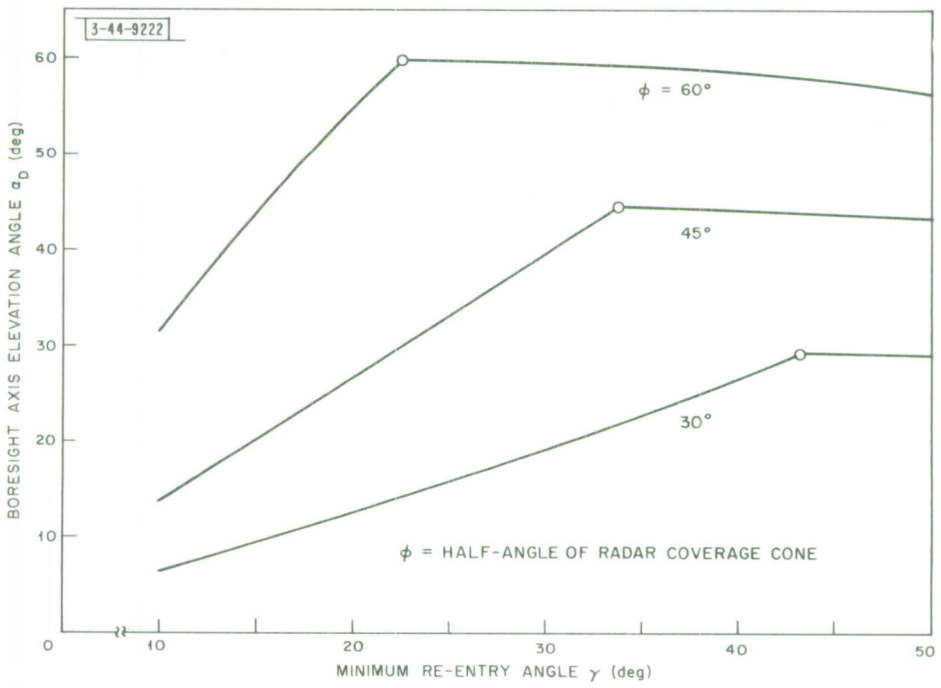

(b) R/h = 0.250.

Fig. 5(a-c). Circular impact-zone boresight axis elevation angle vs minimum re-entry angle.

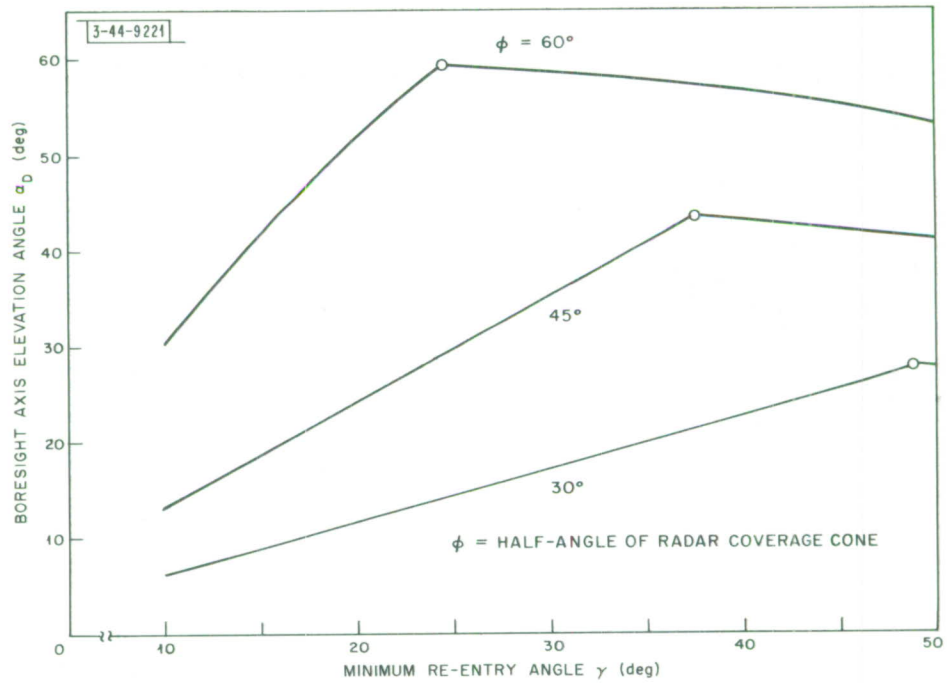

(c) R/h = 0.500.

Fig. 5. Continued.

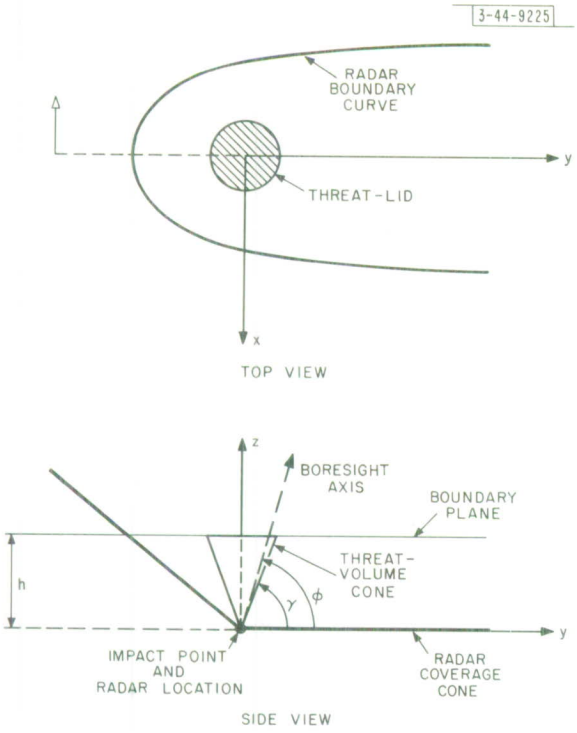

Fig. 6(a). Trivial case, $D_{min} = 0$.

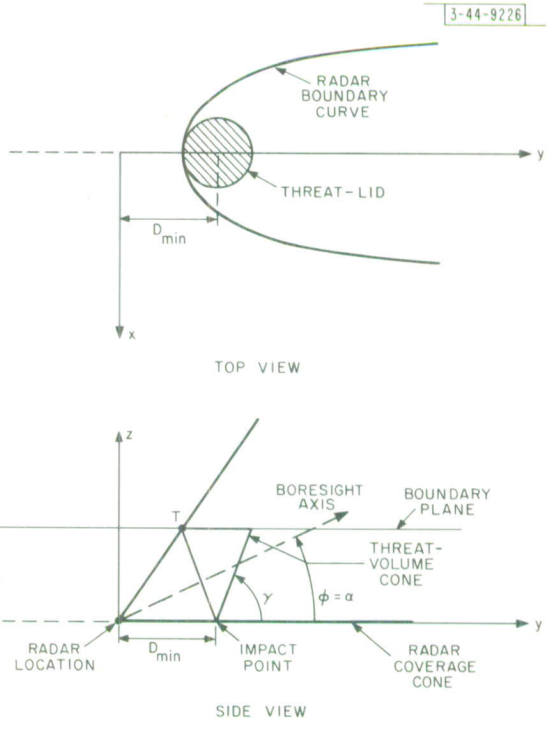

Fig. 6(b). Lip region.

enough to provide the total coverage outlined in the "trivial region." Figure 6(b) illustrates the "lip region" where the threat-lid is small enough to remain internal to the RCBC while having a point T tangential with it at x = 0.

Results:– Table II summarizes point impact-zone mathematical solutions for D_{min}/h and α_D. Figures 7 and 8 show normalized radar location distances (D_{min}/h) and boresight elevation angles (α_D) as a function of the minimum re-entry angle for various maximum radar coverage half-angles (φ). In Figs. 7 and 8, the break points (determined by the value of γ) between regional solutions are indicated by circles. Note that the first derivative of D_{min}/h is continuous at the break points, except for the break point between the "trivial" and "lip" regions.

One can see from Fig. 7 that the minimum radar-to-impact-point distance (D_{min}) is significantly reduced for larger radar scan half-angles. An examination of the 20° re-entry shows a 55-percent reduction in the D_{min} for an increase in radar scan capability (the half-angle φ) from 30° to 60°. This result, which again establishes a definite advantage for a wide scan angle radar system, can be used in trade-off studies to fix the relationship between radar scan capability and other system design parameters such as the transmitter power required.

TABLE II

CASE 2 – FINAL RESULTS FOR THE POINT IMPACT ZONE ($R_o = 0$)

Range of Validity	D_{min}/h	α_D
$(180° - 2\phi) \leqslant \gamma$ "trivial region"	0 (23)	ϕ
$(90° - \phi) \leqslant \gamma \leqslant (180° - 2\phi)$ "lip region"	$(\cot\gamma + \cot 2\phi)$ (22)	ϕ
$\sin^{-1}(\frac{\sqrt{2}}{2}\cos\phi) \leqslant \gamma \leqslant (90° - \phi)$ "tangent region" $R_o = 0$	$\frac{\cot\phi}{2\sin^2\gamma}$ (21a)	ϕ
$0 \leqslant \gamma \leqslant \sin^{-1}(\frac{\sqrt{2}}{2}\cos\phi)$ "dip region" $R_o = 0$	$\frac{\sqrt{\csc^2\gamma - \sec^2\phi}}{\sin\phi}$ (23a) or $\frac{\cot\alpha_D}{\cos^2\phi}$ (23b)	$\tan^{-1}\left[\frac{\tan\phi\sin\gamma}{\sqrt{\cos^2\phi - \sin^2\gamma}}\right]$ (23c)

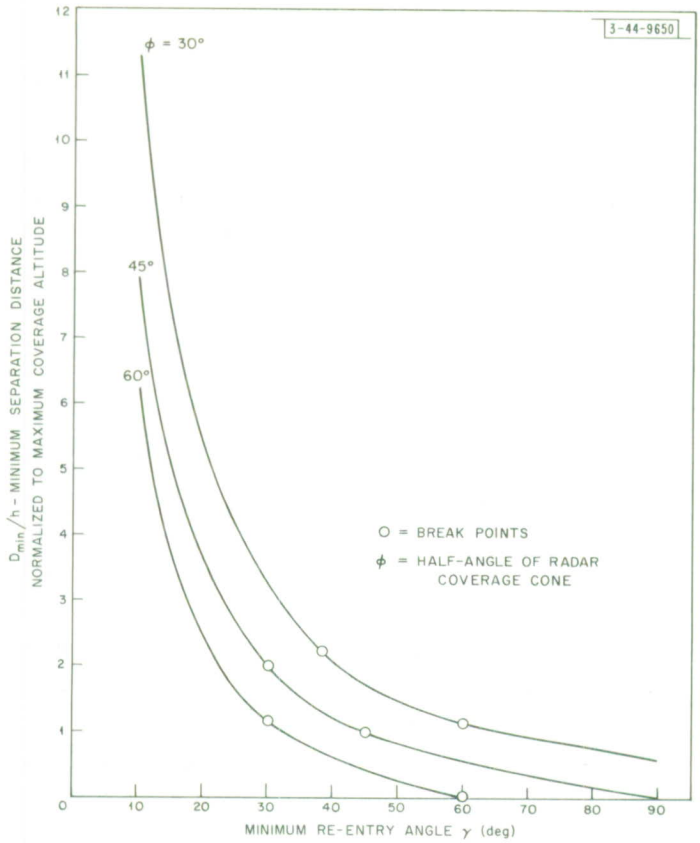

Fig. 7. Point impact-zone case (R = 0) minimum separation distance vs minimum re-entry angle.

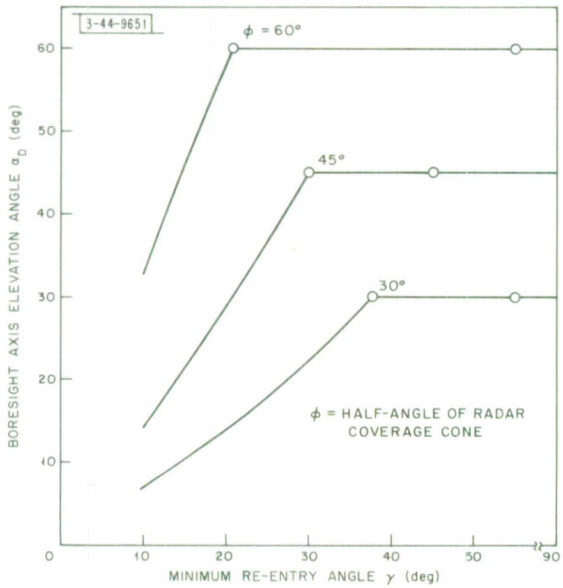

Fig. 8. Point impact-zone case ($D_{min} \neq 0$) minimum boresight axis elevation angle vs minimum re-entry angle.

A. Flat-Earth Approximation

The analysis in Sec. II above is based upon the approximation that the earth is a horizontal plane. If the earth were indeed a flat plane, the results of our analysis would specify the optimum radar location for complete coverage of a particular threat-volume with a specified radar scan capability. However, the earth's surface cannot be represented accurately as a flat plane if the radar site and the threat-volume are located far enough apart for the curvature of the earth to introduce an obstruction. Figure 9(a) illustrates the radar's inability to observe the impact zone and a portion of the threat-volume (the shaded portion of the threat-volume) when this situation exists. Here we will determine the extent of the radar's inability to observe a portion of the threat-volume when the radar site and threat-volume separation distance (D_{min}) is obtained from the preceding analysis in Sec. II.

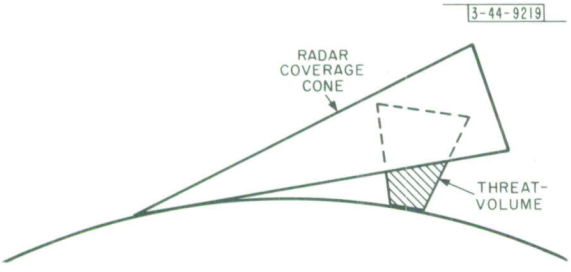

Fig. 9(a). Round-earth geometry.

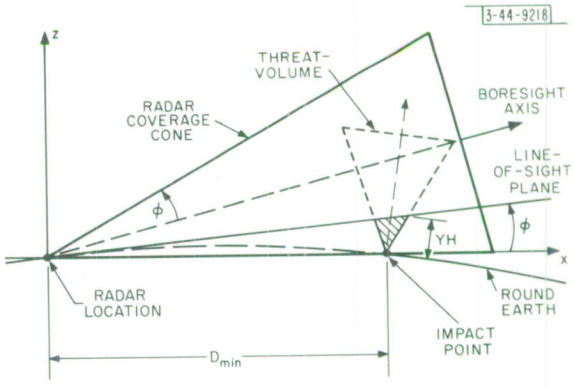

Fig. 9(b). Flat-earth geometry.

From Fig. 9(b), one can see that YH is the minimum altitude above the impact zone for total radar coverage of the threat-volume. The curves of YH in Fig. 10,† for various re-entry angles, may be utilized to determine if the minimum coverage altitude (YH) is acceptable for a particular D_{min}, obtained by applying the flat-earth analysis for the point impact zone ($R_o = 0$). If YH is small enough for a particular radar coverage design problem, the analysis of Sec. II is sufficient. As an example of the radar coverage limitation for a point impact zone, if we let the minimum re-entry angle γ equal 20°, and the radar scan angle φ equal 60°, D_{min}/h will equal 2.45 as shown in Fig. 7. With the aid of Fig. 10, we can construct Table III to show the effect of the earth's curvature in limiting low-altitude coverage. It is apparent from the table that as D_{min} increases, and if we design for extremely high radar coverage acquisition altitudes, YH significantly increases. These results suggest that complete coverage of a threat-volume from very high acquisition altitudes down to the impact zone may require two different radar locations.

In conclusion, the flat-earth approximation will yield useful results. However, the development of the circular and point impact zones in Sec. II is optimum only for the flat-earth model.

† The curves of Fig. 10 are applicable only for the point impact zone ($R_o = 0$). See Appendix E for the YH obtained from considering a circular impact zone.

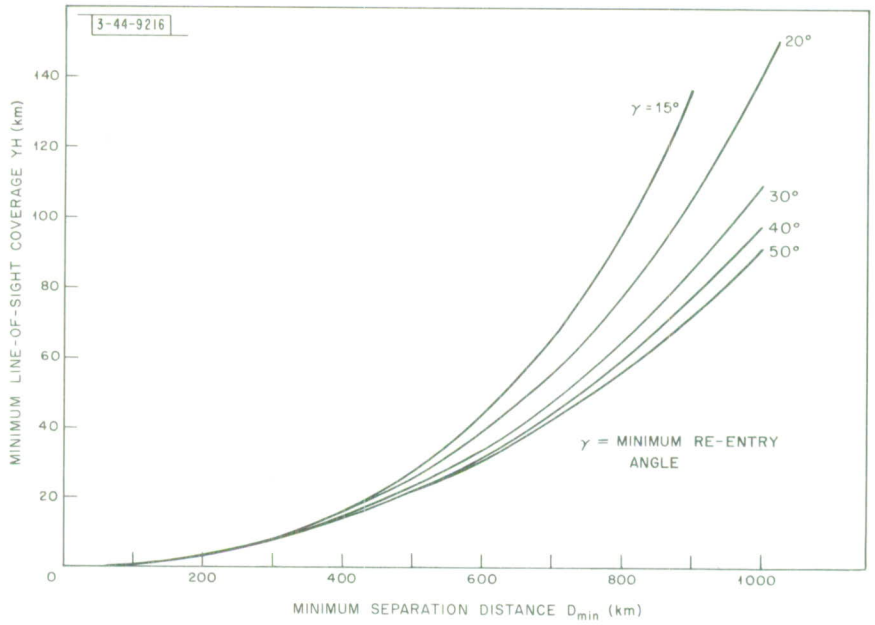

Fig. 10. Minimum line-of-sight coverage for point impact zone (R = 0).

TABLE III

EFFECT OF EARTH'S CURVATURE IN LIMITING LOW-ALTITUDE COVERAGE (For point impact zone, $\gamma = 20°$, $R_o = 0$)

h (km)	D_{min} (km)	YH (km)	YH/h
50	122.5	1.5	0.030
75	184.0	3.0	0.040
100	245.0	5.0	0.050
150	368.0	13.0	0.087
200	490.0	24.5	0.123
250	613.0	40.0	0.160

B. Conclusions

The curves of Figs. 4(a-c) and 7 will allow one to determine rapidly the optimum radar location on a flat earth for representative threats. These curves demonstrate that the minimum separation distance between the radar and the impact-zone center is reduced significantly by utilizing radar systems which are capable of wide scan angles. As a typical example, a 50-percent reduction in separation distance (D_{min}) results for an increase in the radar scan half-angle (φ) from 30° to 60° when $\gamma = 20°$.

The impact-zone size is not of primary importance in determining the separation distance between the radar and impact-zone center. For example, a 100-percent increase in the impact-zone radius will only produce an 11-percent increase in the separation distance, for the typical values of $\varphi = 60°$ and $\gamma = 20°$.

The separation distance between the radar and the impact zone increases significantly as the radar is required to observe higher altitudes. There will be a decrease in the minimum altitude observable by the radar because of the obstruction presented by the earth's curvature.

The curves of Figs. 4(a-c) and 7 can be used to evaluate radar location requirements for more complicated definitions of threat trajectories. For example, if a reduced radar coverage (altitude specification h) is acceptable for low re-entry angle trajectories, then the curves can be used to establish the minimum radar separation distance for low- and high-angle trajectories. The larger of these separations will guarantee the required coverage of the threat-volume. In a manner such as this, the curves can be used to evaluate rapidly a variety of radar coverage requirements.

III. MATHEMATICAL ANALYSIS

Case 1 – Circular Impact Zone ($R_o \neq 0$)

Again considering Figs. 2(a) and (b), one can see that if plane A-B-C-D, which is parallel to the flat earth (x-y plane), is allowed to cut the radar coverage cone at h, the boundary curve of this intersection will either be a parabola (for $\alpha = \varphi$) or a hyperbola (for $\alpha < \varphi$). As previously mentioned, threat-volume average requires that (a) the circular threat-lid boundary and (b) the circular impact zone simultaneously remain internal to the RCBC at the acquisition altitude and on the flat earth (h = 0). Table IV contains the expression for both the parabolic and hyperbolic RCBC together with the first three derivatives and radii of curvature (ρ) for each. The corresponding expressions for the boundary of the circular threat-lid (z = h) and the circular impact zone (z = 0) are given by

$$y_{v\pm} = D \pm \sqrt{R_z^2 - x^2} \tag{1}^{\dagger}$$

$$y'_{v\pm} = \mp \frac{x}{\sqrt{R_z^2 - x^2}} \tag{2}$$

$$\rho_{v\pm} = R_z \tag{3}$$

† The subscript v refers to a position on the circumference of the circular cross section of the threat-volume at height z.

TABLE IV

EXPRESSIONS FOR EDGE OF THE RADAR COVERAGE BOUNDARY CURVE†

	For $\alpha = \phi$	For $\alpha < \phi$
$y_c =$	$\frac{\cot \phi}{2h} x^2 + h \cot 2\phi$	$\frac{\sqrt{x^2 \cos^2 \phi(\cos^2 \alpha - \cos^2 \phi) + h^2 \cos^2 \phi \sin^2 \phi} - (h \sin \alpha \cos \alpha)}{(\cos^2 \alpha - \cos^2 \phi)}$
$y_c' =$	$\frac{\cot \phi}{h} x$	$\frac{x \cos \phi}{\sqrt{x^2(\cos^2 \alpha - \cos^2 \phi) + h^2 \sin^2 \phi}}$
$y_c'' =$	$\frac{\cot \phi}{h}$	$\frac{h^2 \cos \phi \sin^2 \phi}{\left[\sqrt{x^2(\cos^2 \alpha - \cos^2 \phi) + h^2 \sin^2 \phi}\right]^3}$
$y_c''' =$	0	$\frac{-3h^2 x \cos \phi \sin^2 \phi(\cos^2 \alpha - \cos^2 \phi)}{\left[\sqrt{x^2(\cos^2 \alpha - \cos^2 \phi) + h^2 \sin^2 \phi}\right]^5}$
$\rho_c =$	$h \tan \phi \left[1 + (\frac{x}{h})^2 \cot^2 \phi\right]^{3/2}$	$h \tan \phi \left[1 + (\frac{x}{h})^2 \frac{\cos^2 \alpha}{\sin^2 \phi}\right]^{3/2}$

Note: $\rho_c = \left| \frac{[1 + (y_c')^2]^{3/2}}{y_c''} \right|$.

† See Appendix A for derivation of y_c for $\alpha < \phi$. The subscript c refers to a position on the radar coverage boundary curve.

where

$$\left.\begin{aligned} R_z &= R(z) = z \cot\gamma + R_o \\ y_v &= y(x, z) \end{aligned}\right\} \quad \text{for } x \geqslant 0 \quad \text{and} \quad 0 \leqslant z \leqslant h \quad .$$

Only one condition, which is both sufficient and necessary, must be met if the threat-volume is to be covered completely by the radar coverage cone. This condition is expressed by the inequality

$$x_c^2(y_z) - x_v^2(y_z) \geqslant 0 \tag{4}$$

where

$$y_z = y_v(z) = y_c(z) \quad .$$

If we let

$$U(y_z) = x_c^2(y_z) - x_v^2(y_z) \tag{5}$$

this implies that

$$U(y_z) \geqslant 0 \quad \text{for all } 0 \leqslant z \leqslant h \quad . \tag{6}$$

Because of the convexity of the radar conical scan region, a radar which can cover simultaneously the threat-lid and the impact-zone circular boundary curves will also cover the entire threat-volume as shown in Fig. 1. This follows because any point in the threat-volume lies on some straight-line segment between a point on the threat-lid and one in the impact zone. Therefore, the point is internal to the radar scan coverage region if the two circular boundaries are internal to the radar coverage boundaries. Equation (6) now can be reduced to

$$U(y_z) \geqslant 0 \quad \text{for } z = 0, h \quad . \tag{7}$$

The minimum radar location D_{min} can be obtained by finding the y which causes $U(y)$ to be a minimum; that is, solving for the y from

$$\frac{dU(y)}{dy} = 0 \quad . \tag{8}$$

The expression in Table IV for y_c, where $\alpha < \varphi$, can be written in the form

$$x_c^2 = Ay_c^2 + By_c + C \tag{9}^{\dagger}$$

where A, B, and C are functions of z.

By utilizing Eqs. (1), (9), and (5), we can obtain $U(y_z)$.

$$U(y_z) = (A + 1)\, y^2 + (B - 2D)\, y + C - R_z^2 + D^2 \tag{10}$$

where

$$z = 0, h$$

† See Appendix A, Eq. (A-1).

for use in Eq.(8), thereby yielding

$$y_{min} = \frac{2D - B}{2(A + 1)} \quad . \tag{11}$$

U_{min}, which is obtained from Eqs.(10) and (11), is given by

$$U_{min} = -\frac{(2D - B)^2}{4(A + 1)} + C - R_z^2 + D^2 \tag{12}$$

where

$$z = 0, h \quad .$$

The expression for U_{min} (hereafter referred to as U_m) must satisfy the inequality (7) for both threat-lid (z = h) and impact-zone (z = 0) coverage. Because (7) is an inequality, the limits must be properly chosen to assure that D is a minimum; this selection of limits can possibly be made by considering Fig. 1 where it can be seen that D will be a minimum when the circular threat-lid is tangent to the edge of the RCBC. This follows because the radar coverage cone is as close to the threat-lid without any portion of the threat-lid extending outside the RCBC. These conditions are expressed by

$$\left.\begin{array}{ll} \text{(a)} & y'_{v-}(\pm x) = y'_c(\pm x) \quad \text{when } x = a \\ \text{(b)} & y_{v\pm}(x) \geqslant y_c(x) \\ \text{(c)} & \rho_v(x) \leqslant \rho_c(x) \end{array}\right\} \quad \text{for } D > 0,\ \alpha \leqslant \varphi \quad . \tag{13}$$

The condition of Eq.(4) will be the most general restriction, satisfy Eq.(13), and yield D_{min} if and only if U_m (lid) = 0 at the threat-lid (z = h).

Coverage of the circular impact zone is specified by two regional solutions. In the first region, the RCBC is tangent to the impact-zone circular boundary curve (at z = 0) and the conditions of Eq.(13) apply for z = 0, thereby satisfying Eq.(4) where U_m (base) = 0 must again hold. The second region only satisfies conditions (a) and (b) of Eq.(13) and therefore causes U_m (base) > 0 to hold. This case is equivalent to a small enough impact-zone radius that threat-lid coverage assures adequate coverage of the impact zone. These solutions can be summarized by

$$\text{Region 1} \quad U_m(\text{lid}) = 0 \quad \text{and} \quad U_m(\text{base}) = 0 \tag{14}$$

$$\text{Region 2} \quad U_m(\text{lid}) = 0 \quad \text{and} \quad U_m(\text{base}) > 0 \tag{15}$$

where

$$U_m(\text{lid}) = U_m\big|_{z=h} \quad \text{and} \quad U_m(\text{base}) = U_m\big|_{z=0} \quad .$$

The determination of when to use each case can be related to the design parameters α, R_o, φ, and h by solving for the value of γ where region 1 applies – that is, where Eqs.(4) and (13) must be satisfied. If γ is less than a critical value γ^*, then region 2 and Eq.(15) can be utilized where the threat-lid is optimumly covered and the impact zone is more than covered. The critical value γ^* is obtained by considering the impact-zone subtended half-angle β_c [see Fig. 11(a)] when the conditions of Eqs.(13) and (4) are satisfied. This limiting case yields

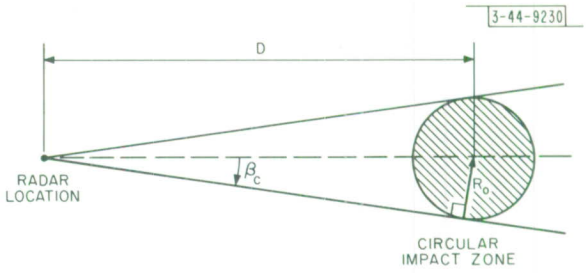

Fig. 11(a). Ground plane view of circular impact zone for RCBC.

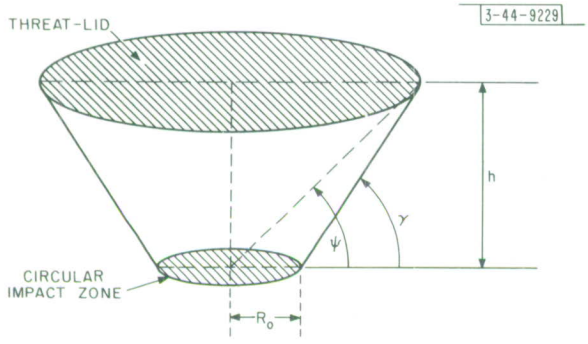

Fig. 11(b). Threat-volume geometry showing angular variation for Eq. (17).

$$\sin\beta_c = \left.\frac{R_o}{D_{min}}\right|_{\gamma=\gamma^*} \tag{16a}$$

where, upon solving for γ^*, results in

$$\gamma^* = \cot^{-1}\left(\sqrt{2\sec^2\varphi + r^2 - 1} - r\right) \tag{16b}^{\dagger}$$

when we utilize the relationships [see Fig. 11(b)]

$$\cot\psi^* = \cot\gamma^* + r \tag{17}$$

$$r = \frac{R_o}{h} \quad . \tag{18}$$

The minimum value of D can now be obtained for each of the two cases.

Region 1, $\gamma^* < \gamma < 90°$:– In the "tangent region," by utilizing Eq. (12) with Eq. (14) and solving for D, we obtain

$$D_{min} = h\csc\varphi\left\{r^2 + \left[\frac{(\cot\gamma + r)^2 + 1 - r^2}{2\sec\varphi}\right]^2\right\}^{1/2} \tag{19a}$$

$$\alpha_D = \cot^{-1}\left\{\cot^2\varphi + \left[\frac{2r\csc\varphi}{(\cot\gamma + r)^2 + 1 - r^2}\right]^2\right\}^{1/2} \quad . \tag{19b}$$

Region 2, $0 < \gamma \leqslant \gamma^*$:– In this region, designated the "dip region," the solution for D_{min} and α_D which satisfy Eqs. (12) and (15) is given by

† See Appendix B.

$$D_{min} = \frac{h\sqrt{(\cot\gamma + r)^2 - \tan^2\varphi}}{\sin\varphi} \qquad (20a)^{\dagger}$$

or

$$D_{min} = \frac{h \cot\alpha_D}{\cos^2\varphi} \qquad (20b)$$

$$\alpha_D = \tan^{-1}\left[\frac{\tan\varphi}{\cos\varphi\sqrt{(\cot\gamma + r)^2 - \tan^2\varphi}}\right] \quad . \qquad (20c)$$

The expressions for D_{min} and α_D for the circular impact zone are given in Table I.

Case 2 – Point Impact Zone ($R_o = 0$)

For a point impact zone ($R_o = 0$), a few special cases result which are not only of interest but improve the generality of the overall solution. These special cases result from the "tangent region" and the "dip region" of the general solution for the circular impact zone by letting $R_o = 0$.

"Tangent Region ($R_o = 0$)":– The expressions for D_{min} and α_D, which are obtained from Eqs. (19a) and (19b) by setting $R_o = 0$, are given by

$$\left.\begin{aligned} D_{min} &= h\,\frac{\cot\varphi}{2\sin^2\alpha} \qquad (21a) \\ \alpha_D &= \varphi \qquad (21b) \end{aligned}\right\} \quad \sin^{-1}\left(\frac{\sqrt{2}}{2}\cos\varphi\right) \leqslant \gamma \leqslant (90° - \varphi) \quad .$$

If the threat-lid is small enough to be wholly internal to the RCBC and has only one point of tangency at x = 0 [see Fig. 10(b)], the solution for D_{min} results in

$$D_{min} = h(\cot\gamma + \cot 2\varphi) \quad \text{for } \alpha_D = \varphi \qquad (22)$$

when

$$(90° - \varphi) \leqslant \gamma \leqslant (180° - 2\varphi) \quad .$$

The angular ranges for γ are obtained by utilizing condition (c) of Eq. (13) at x = 0, which implies

$$\rho_{v-}\big|_{x=0} \leqslant \rho_c\big|_{x=0}$$

$$h \cot\gamma \leqslant h \tan\varphi$$

where, upon solving the inequality, gives the following results

$$(90° - \varphi) \leqslant \gamma \quad .$$

If D_{min} is set equal to zero [see Fig. 6(a)] in Eq. (22), the larger angular limit for γ which can be solved for results in

$$D = 0 = h(\cot\gamma + \cot 2\varphi)$$

$$\gamma = (180° - 2\varphi) \quad . \qquad (23)$$

† See Appendix D for derivation.

When $\gamma \geqslant (180° - 2\varphi)$, D_{min} equal zero is obviously a trivial case. [Note: $D = 0$, $180° - (\varphi + \gamma) \leqslant \alpha \leqslant (\varphi + \gamma)$ is a singular point solution in the range $(90° - \varphi) \leqslant \gamma \leqslant (180° - 2\varphi)$; i.e., there is no solution for $0 < D < D_{min}$. Therefore, this trivial solution will be ignored to yield a continuous function of $D_{min}(\alpha)$.]

"Dip Region ($R_o = 0$)":– If $R_o = 0$ in Eqs.(20a) through (20c), D_{min} and α_D are given by

$$D_{min} = \frac{h\sqrt{\csc^2\gamma - \sec^2\varphi}}{\sin\varphi} \qquad (23a)$$

or

$$D_{min} = \frac{h \cot\alpha_D}{\cos^2\varphi} \qquad (23b)$$

$$0 < \gamma \leqslant \sin^{-1}\left(\frac{\sqrt{2}}{2}\cos\varphi\right) \quad .$$

where

$$\alpha_D = \tan^{-1}\left(\frac{\tan\varphi \sin\gamma}{\sqrt{\cos^2\varphi - \sin^2\gamma}}\right) \qquad (23c)$$

Table III, which is a summary of the special cases for the point impact zone ($R_o = 0$), contains expressions for D_{min}/h, α_D, and their range of validity as controlled by γ.

APPENDIX A
HYPERBOLIC BOUNDARY CURVE
(Derivation of equation for y_c in Table IV for $\alpha < \varphi$)

Visual reference: Fig. 2(a).

Let

$\overline{B}$ = a unit vector along the boresight axis (0 to ba)

$\overline{T}$ = a unit vector from point 0 to the cone and plane intersection, thereby describing the boundary.

From Fig. 2(a), note that the following are true:

$\overline{B} = (0, \cos\alpha, \sin\alpha)$

$\overline{T} = (x, y_c, h)$.

Therefore,

$$\cos\varphi = \frac{\overline{B} \cdot \overline{T}}{|\overline{B}|\,|\overline{T}|}$$

$$= \frac{y_c \cos\alpha + h \sin\alpha}{\sqrt{x^2 + y_c^2 + h^2}} \quad .$$

Upon simplification, one obtains

$$y_c = \frac{\sqrt{x^2 \cos^2\varphi(\cos^2\alpha - \cos^2\varphi) + h^2 \cos^2\varphi \sin^2\varphi} - (h \cos\alpha \sin\alpha)}{(\cos^2\alpha - \cos^2\varphi)} \quad . \qquad (A\text{-}1)$$

APPENDIX B
CRITICAL RE-ENTRY ANGLE γ^*
[Derivation of Eq. (16b) for γ^*]

Utilizing Eq. (16a),

$$\sin\beta_c = \frac{R_o}{D_{min}\big|_{\gamma=\gamma^*}}$$

and the result of Appendix C

$$\cos^2\beta_c = \frac{\cos^2\varphi}{\cos^2\alpha}$$

$$\sqrt{1-\cos^2\beta_c} = \sqrt{1-\frac{\cos^2\varphi}{\cos^2\alpha}} = \sin\beta_c = \frac{R}{D_{min}\big|_{\gamma=\gamma^*}} \quad . \tag{B-1}$$

Since we are using the "dip region" for threat-lid coverage from Case 1 [Eq. (20a)] and the notation change of Eq. (17), then D_{min} can be written

$$D_{min}\big|_{\gamma=\gamma^*} = \frac{h\sqrt{\csc^2\psi^* - \sec^2\varphi}}{\sin\varphi} \quad . \tag{B-2}$$

By equating (B-1) and (B-2), we obtain

$$\sqrt{1-\frac{\cos^2\varphi}{\cos^2\alpha}} = \frac{R_o}{D_{min}\big|_{\gamma=\gamma^*}} = \frac{R_o\sin\varphi}{h\sqrt{\csc^2\psi^* - \sec^2\varphi}} \quad .$$

Solving for $\cot\psi^*$ in order to use Eq. (17) to obtain γ^*, we must labor through the following:

$$1-\frac{\cos^2\varphi}{\cos^2\alpha} = \frac{r^2\sin^2\varphi}{(\csc^2\psi^* - \sec^2\varphi)} \qquad \text{where } r = \frac{R_o}{h}$$

$$(\csc^2\psi^* - \sec^2\varphi)\,[1-\cos^2\varphi(1+\tan^2\alpha)] = r\sin^2\varphi \quad .$$

To eliminate α, we use Eqs. (20c) and (17) thereby obtaining

$$\alpha = \tan^{-1}\left(\frac{\tan\varphi\,\sin\psi^*}{\sqrt{\cos^2\varphi - \sin^2\psi^*}}\right)$$

$$(\csc^2\psi^* - \sec^2\varphi)\left\{1-\cos^2\varphi\left[1+\frac{\tan^2\varphi\,\sin^2\psi^*}{(\cos^2\varphi - \sin^2\psi^*)}\right]\right\} = r^2\sin^2\varphi$$

$$\left[\frac{\cos^2\varphi - \sin^2\psi^*}{\sin^2\psi^*\cos^2\varphi}\right]\left\{1-\cos^2\varphi\left[\frac{\cos^2\varphi + \sin^2\psi^*(\tan^2\varphi - 1)}{\cos^2\varphi - \sin^2\psi^*}\right]\right\} = r^2\sin^2\varphi \quad .$$

By using squared trigonometric identities and simplifying, we obtain

$$\cos^2\varphi = \sin^2\psi^*(r^2\cos^2\varphi + 2) \quad .$$

It follows that

$$\csc^2\psi^* = r^2 + 2\sec^2\varphi = 1 + \cot^2\psi^*$$

$$\cot^2\psi^* = r^2 + 2\sec^2\varphi - 1 \quad .$$

From Eq.(17), we obtain

$$\cot\gamma^* = -r \pm \sqrt{r^2 + 2\sec^2\varphi - 1}$$

where the negative radical solution can be eliminated since γ^* must be in the first quadrant. Therefore,

$$\gamma^* = \cot^{-1}\left(\sqrt{2\sec^2\varphi + r^2 - 1} - r\right) \quad .$$

APPENDIX C
COSINE PRODUCT IDENTITY
(Derivation of identity used in Appendix B)

Visual reference: Fig. C-1.

Let

ℓ = altitude of radar cone

r_c = radius of radar cone base circle at cone altitude ℓ

β_c = angle subtended by cone intersection with x-y plane and y-axis

s_1 and b_1 are shown in Fig. C-1.

From the figure, note that the following are true: $\cos\alpha = \ell/s_1$; $\tan\varphi = r_c/\ell$; $\tan\beta_c = R_o/s_1$; $\tan\alpha = b_1/\ell$. Consider the right triangle formed by r_c, R_o, and b_1

$$r_c^2 = R_o^2 + b_1^2$$

$$(\ell \tan\varphi)^2 = (s_1 \tan\beta_c)^2 + (\ell \tan\alpha)^2$$

$$= (\tan^2\beta_c)(\ell^2 \sec^2\alpha) + (\ell \tan\alpha)^2$$

$$\tan^2\varphi = \tan^2\beta_c \sec^2\alpha + \tan^2\alpha$$

making use of squared identities

$$(\sec^2\varphi - 1) = \sec^2\alpha(\sec^2\beta_c - 1) + (\sec^2\alpha - 1)$$

$$\sec^2\varphi = \sec^2\alpha \sec^2\beta_c$$

$$\cos\varphi = \cos\alpha \cos\beta_c$$

therefore,

$$\cos\beta_c = \cos\varphi/\cos\alpha \quad .$$

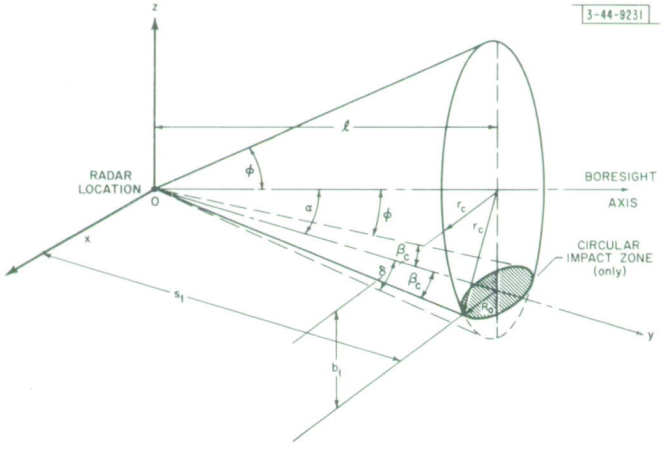

Fig. C-1. Radar coverage of circular impact zone.

APPENDIX D

"DIP REGION" SOLUTION FOR D_{min} AND α_D

[Derivation of Eqs. (20a) and (20b)]

Visual reference: Figs. 3(a) and (b).

If we utilize condition (a) of Eq. (13), Eq. (2), and y_c for $\alpha < \varphi$ from Table IV, the x coordinates ($\pm a$) of the tangent points in Fig. 3(a) can be found from

$$y'_{v-}(a) = y'_c(a)$$

$$\frac{a}{\sqrt{h^2(\cot\gamma + r)^2 - a^2}} = \frac{a\cos\varphi}{\sqrt{a^2(\cos^2\alpha - \cos^2\varphi) + h^2\sin^2\varphi}}$$

to be

$$a = \pm h\,\frac{\cos\varphi}{\cos\alpha}\sqrt{(\cot\gamma + r)^2 - \tan^2\varphi} \quad . \tag{D-1}$$

The length of the boresight axis, ℓ [side view of Fig. 3(b)] between the radar location (0, 0, 0) and its intersection the threat-lid (0, b, h) is given by

$$\ell = h\csc\alpha \quad . \tag{D-2}$$

The following relation can be obtained from the triangle formed by the coordinates (a, b, h), (0, 0, 0), and (0, b, h)

$$a = \ell\tan\varphi \quad . \tag{D-3}$$

If Eqs. (D-1), (D-2), and (D-3) are combined, an expression for α can be found

$$\tan\alpha_D = \frac{\tan\varphi}{\cos\varphi\sqrt{(\cot\gamma + r)^2 - \tan^2\varphi}} \quad . \tag{D-4}$$

D_{min} can be written from inspection of Fig. 3(b) as

$$D_{min} = h\cot\alpha + \sqrt{h^2(\cot\gamma + r)^2 - a^2} \tag{D-5}$$

where Eqs. (D-1) and (D-4) can be used to reduce Eq. (D-5) to

$$D_{min} = \frac{h\sqrt{(\cot\gamma + r)^2 - \tan^2\varphi}}{\sin\varphi} \quad . \tag{D-6}$$

If Eqs. (D-6) and (D-4) are substituted into Eq. (15), the relationship for U_m (lid) is equal to zero.

APPENDIX E
MINIMUM COVERAGE DEVELOPMENT

Let

R_o = radius of circular impact zone

M = radius of the earth

YH = minimum coverage height.

I. POINT IMPACT ZONE

The following relationships are obtained by considering the individual triangles of Fig. E-1:

Triangle ODL

$$Z = M(\sec\Theta - 1) \tag{E-1}$$

Triangle ABI

$$YH = X\tan\gamma \tag{E-2}$$

Triangle ABL

$$(YH - Z) = X\tan\Theta \tag{E-3}$$

Triangle DOI

$$D_{min} = 2M\sin(\Theta/2) \tag{E-4}$$

where

$$\Theta = \cos^{-1}\left[1 - \frac{1}{2}\left(\frac{D_{min}}{M}\right)^2\right] \quad . \tag{E-5}$$

Equation (E-5) is an alternate form of Eq. (E-4) obtained by using half-angle identities.

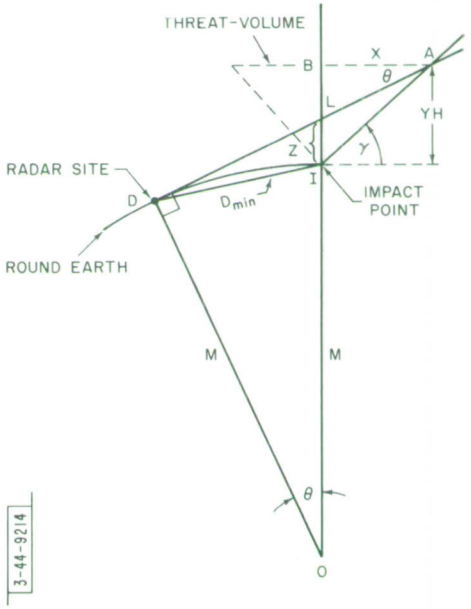

Fig. E-1. Limiting coverage geometry for point impact zone.

By dividing Eq. (E-2) into Eq. (E-3), we obtain

$$\frac{Z}{YH} = 1 - \frac{\tan\Theta}{\tan\gamma}$$

$$YH = \frac{Z \tan\gamma}{\tan\gamma - \tan\Theta} \quad . \tag{E-6}$$

Utilizing Eq. (E-1),

$$YH = \frac{M(\sec\Theta - 1)\tan\gamma}{\tan\gamma - \tan\Theta} \quad . \tag{E-7}$$

By multiplying the numerator and denominator by $(\cos\gamma \cos\varphi)$, we obtain

$$YH = \frac{M(1 - \cos\Theta)\sin\gamma}{\sin\gamma\cos\Theta - \sin\Theta\cos\gamma} \tag{E-8a}$$

$$= \frac{M(1 - \cos\Theta)\sin\gamma}{\sin(\gamma - \Theta)} \quad . \tag{E-8b}$$

Combining Eqs. (E-5) and (E-8a) yields

$$YH = \frac{D_{min}^2 \sin\gamma}{2M(\sin\gamma\cos\Theta - \sin\Theta\cos\gamma)} \tag{E-9}$$

where

$$\Theta = \cos^{-1}\left[1 - \frac{1}{2}\left(\frac{D_{min}}{M}\right)^2\right] \quad . \qquad \text{[Eq. (E-5)]}$$

These results can be simplified for rapid calculations by making use of the small angle approximations for Θ.

For small Θ,

$$\cos\Theta \approx 1 \quad \text{and} \quad \sin\Theta \approx \frac{D_{min}}{M}$$

therefore,

$$YH \approx \frac{0.5D_{min}^2 \sin\gamma}{M\sin\gamma - D_{min}\cos\gamma} \quad . \tag{E-10}$$

II. CIRCULAR IMPACT ZONE

The following relationships are obtained by considering the individual triangles of Fig. E-2:

Triangle WEI

$$P = R_o \tan\gamma \tag{E-11}$$

Triangle ABL

$$(YH - Z) = X\tan\Theta \qquad \text{[Eq. (E-3)]}$$

Triangle ABW

$$(YH + P) = X\tan\gamma \tag{E-12}$$

Triangle ODL

$$Z = M(\sec\Theta - 1) \quad . \qquad \text{[Eq. (E-1)]}$$

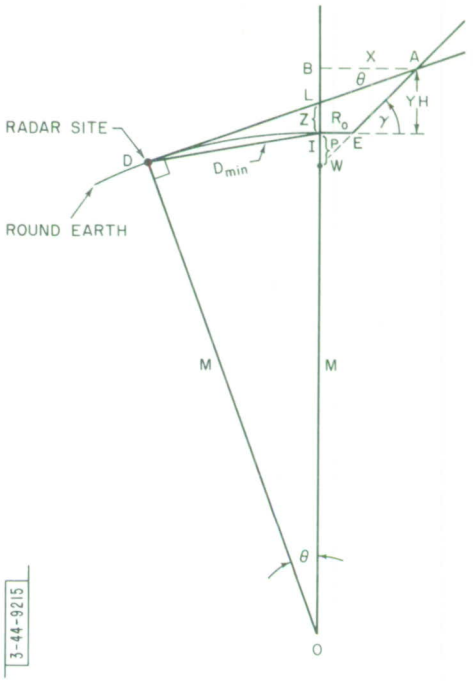

Fig. E-2. Limiting coverage geometry for circular impact zone.

By dividing Eq. (E-3) by Eq. (E-12), we obtain

$$\frac{YH - Z}{YH - P} = \frac{\tan\Theta}{\tan\gamma}$$

satisfying

$$YH = \frac{Z \tan\gamma + P \tan\Theta}{\tan\gamma - \tan\Theta} \quad . \tag{E-13}$$

By utilizing Eqs. (E-1), (E-5), and (E-11) and by multiplying the numerator and denominator by $(\cos\gamma \cos\Theta)$, we obtain

$$YH = \frac{\left(\frac{D_{min}^2}{2M} + R_o \sin\Theta\right) \sin\gamma}{\sin\gamma \cos\Theta - \sin\Theta \cos\gamma} \tag{E-14}$$

where

$$\Theta = \cos^{-1}\left[1 - \frac{1}{2}\left(\frac{D_{min}}{M}\right)^2\right] \quad . \qquad \text{[Eq. (E-5)]}$$

Once again, small angle approximation may be used on Eq. (E-14) to obtain

$$YH \approx \frac{[0.5D_{min} + R_o] \sin\gamma}{\frac{M \sin\gamma}{D_{min}} - \cos\gamma} \quad . \tag{E-15}$$

ACKNOWLEDGMENTS

The authors are indebted to J. Resnick for his comments and suggestions in the initial phases of this work. Appreciation is also expressed to W. P. Delaney for his continued interest and many valuable suggestions. We are also indebted to Dr. H. Schneider and H. J. Pratt for their review of the manuscript and to S. D. Weiner for his suggestions concerning the mathematical derivations.

DOCUMENT CONTROL DATA – R&D

(Security classification of title, body of abstract and indexing annotation must be entered when the overall report is classified)

1. ORIGINATING ACTIVITY *(Corporate author)*
Lincoln Laboratory, M.I.T.

2a. REPORT SECURITY CLASSIFICATION
Unclassified

2b. GROUP
None

3. REPORT TITLE
Radar Location for Complete Coverage of Representative Threat-Volumes

4. DESCRIPTIVE NOTES *(Type of report and inclusive dates)*
Technical Report

5. AUTHOR(S) *(Last name, first name, initial)*
Ewing, Samuel D., Jr. Caldwell, David

6. REPORT DATE
15 August 1966

7a. TOTAL NO. OF PAGES
40

7b. NO. OF REFS
None

8a. CONTRACT OR GRANT NO.
AF 19(628)-5167

b. PROJECT NO.
ARPA Order No. 498

c.

d.

9a. ORIGINATOR'S REPORT NUMBER(S)
Technical Report 422

9b. OTHER REPORT NO(S) *(Any other numbers that may be assigned this report)*
ESD-TR-66-413

10. AVAILABILITY/LIMITATION NOTICES
Distribution of this document is unlimited.

11. SUPPLEMENTARY NOTES
None

12. SPONSORING MILITARY ACTIVITY
Advanced Research Projects Agency, Department of Defense

13. ABSTRACT

A radar is constrained to scan within a volume of space modeled as a cone with the apex at the radar. The threat-volume is modeled as the frustum of a right-circular cone inverted on a flat earth with a vertical axis and with the height equal to the maximum acquisition altitude. Threatening objects can enter anywhere within this volume above some specified minimum re-entry angle that determines the apex angle of the frustum. The problem solved is that of finding the minimum surface range of the radar that permits the entire frustum volume to be included within the given scanning cone. The important special case of a point impact zone (base radius of frustum $\rightarrow 0$) is also discussed. Results are presented showing how this minimum distance is affected by changing (1) the minimum re-entry angle, (2) the scan angle, (3) the maximum radar acquisition altitude, and (4) the impact-zone radius. Effects of earth curvature are also discussed. These results are useful as one aspect of optimizing radar location in terminal defense studies.

14. KEY WORDS

threat-volume
impact studies
terminal defense
ballistic missiles
radar location
re-entry vehicles
re-entry trajectories
radar antennas